Synthesis of SiO_2 and SnO_2 Particles in Diffusion Flame Reactors

Wenhua Zhu and Sotiris E. Pratsinis
Dept. of Chemical Engineering, University of Cincinnati, Cincinnati, OH 45221

Silica and stannic (tin) oxide powders were synthesized by oxidation of their respective chlorides in single and double (inverse) diffusion flame reactors. The effect of reactant gas mixing on the characteristics of these powders (size and morphology) was investigated by altering the position of the fuel (CH_4) and oxidant (air or O_2) streams in the burner. Reactant gas mixing plays a key role in controlling particle size since it affects the temperature history, residence time, and initial particle concentration in the flame, thus, yielding a simple technique for particle-size control over a wide size range in flame reactors. The different material properties (such as sintering) of silica and stannic oxide result in particles of different size and morphology, although they were made at nearly identical flame conditions. Moreover, the oxidant composition affects significantly the properties of silica particles.

Introduction

Flame reactors are routinely used to make submicron particles on an industrial scale, the most important of which are carbon black, fumed silica, and titania (Ulrich and Riehl, 1982). Flame processes are advantageous for producing materials of high purity at high yield since they do not involve the tedious steps, high liquid volumes, and surfactants needed by wet chemistry processes (Pratsinis and Mastrangelo, 1989). The control of particle growth during flame synthesis is crucial since the properties of materials made with these particles depend on size distribution, morphology, extent of agglomeration, and chemical and phase composition of the starting powders. For example, in the manufacture of titania pigments, the objective is to produce nearly monodisperse rutile phase particles lying between 150 ~ 250 nm to obtain the maximum hiding power per unit mass (Clark, 1975). In contrast, in the manufacture of titania powders for photocatalysts, ultrafine (25 ~ 50 nm) and mostly anatase phase particles are needed to provide a large density of active sites (Fotou et al., 1994a).

It is known that flame temperature, residence time, and precursor concentration are key variables that determine final particle size and phase composition of flame made powders (Ulrich, 1971; Formenti et al., 1972; Pratsinis, 1997). Besides, the presence of additives or dopants (Fotou et al., 1995; Vemury and Pratsinis, 1995a), electrical charging (Vemury and Pratsinis, 1995b), and reactant gas mixing (Pratsinis et al., 1996) can significantly affect the characteristics of the product powders. Doping, however, introduces undesirable impurities and charging adds cost to the products.

Zachariah and Huzarewicz (1991) first reported that flame configuration may have a profound effect on the product powder properties. Specifically, they made submicron $YBa_2Cu_3O_7$ particles by pyrolysis of the corresponding aqueous nitrate salts in oxy-hydrogen flames. They found that using an overventilated co-flow diffusion flame resulted in superconducting powders while these powders cannot be obtained when a premixed flame configuration was used. Du and Axelbaum (1995) recently pointed out that the gas mixing configuration could affect the flame structure and thus the soot particle inception in coannular diffusion flames. When nitrogen was separated from the air feed and added to the fuel stream, or in other words, when flame configuration was changed from fuel/air flame to diluted-fuel/oxygen flame, the flame front shifted towards the fuel side (center) and soot formation was suppressed by the change in fuel pyrolysis and oxidation rates adjacent to the pyrolysis zone. It should be emphasized that the adiabatic temperatures of both flames were identical.

The effect of flame configuration on TiO_2 particle size and phase composition was investigated by altering the positions

Correspondence concerning this article should be addressed to S. E. Pratsinis.

of methane and air streams in a diffusion flame reactor (Pratsinis et al., 1996). Without changing any of the flow rates, the average primary particle size of TiO_2 can be controlled from 11 to 105 nm by merely altering the reactant mixing configuration. Nonagglomerate, perfectly spherical titania particles up to 250 nm in diameter can be made in diffusion flame reactors when oxygen is used as oxidant (Zhu and Pratsinis, 1996). Material properties are crucial also in flame synthesis of powders as Matsoukas and Friedlander (1991) showed that the primary particle size of ZnO is two to four times larger than that of MgO even though nearly identical premixed flames are used for synthesis of these powders.

In the present study, standard single and double coflow diffusion flames are characterized and their effects on synthesis of SiO_2 and SnO_2 powders are closely investigated as diffusion flames are used on an industrial scale for powder production. These materials are examined for their significance in manufacture of fumed silica or optical fibers (SiO_2), as well as for their potential for synthesis of films and sensors (SnO_2). From a fundamental point of view, these two materials have significantly different properties (such as sintering mechanisms) allowing a broader examination of the effect of reactant gas mixing on powder production in flames. In addition, the effect of oxidant composition on the characteristics of these powders is investigated.

Experimental Studies

A diffusion flame burner is used here since it provides a stable flame over a wide range of operating conditions (Fotou et al., 1994). Particle formation is studied in a diffusion flame reactor consisting of a series of concentric quartz tubes. The central tube of the reactor is 0.5 cm in diameter while the wall thickness and spacing between successive tubes is 0.1–0.2 cm. A detailed description of the apparatus can be found in Pratsinis et al. (1996).

Methane (Wright Brothers, 99%) is used as fuel while dry air or oxygen (Wright Brothers, 99.9%) is used as oxidant. The precursor vapor ($SiCl_4$ or $SnCl_4$) is carried into the central tube of the reactor by passing dry argon gas (Wright Brothers, 99.8%) through a bubbler containing the corresponding metallic chloride in liquid phase so the Ar stream was always saturated with the precursor as determined gravimetrically. The temperature of the liquid precursor is kept at 49° and 0°C for $SnCl_4$, and $SiCl_4$, respectively, in order to maintain identical precursor flowing rate, 1.0×10^{-3} mol/min. At these temperatures, the vapor pressure of $SiCl_4$ is 76.2 mm Hg and that of $SnCl_4$ is 76.6 mm Hg (Weast, 1983). The reactor and manifold temperatures are kept about 20°C above liquid precursor temperatures to avoid condensation of the precursor vapor. All reactant flow rates are controlled by calibrated rotameters (Zhu, 1996). The flow rates of methane and argon are maintained at 400 cm^3/min and 250 cm^3/min, respectively, at room temperature (23°C) in all experiments. Temperatures are measured by thermocouples except for the liquid precursor temperatures, which are measured by thermometers.

Particles are formed in the flame by precursor oxidation/hydrolysis (Bautista and Atkins, 1991) and collected on glass fiber filters (Gelman Scientific; 143 mm) by the aid of a vacuum pump. The filter cased inside a cylinder chimney is held 120 mm above the burner face so that the temperature at the filter would not exceed 300°C throughout the experiments. Corrosive byproducts such as Cl_2 and HCl are removed from the exhaust by passing them through a 1M NaOH aqueous solution before being released to the fume hood.

The specific surface area of the powders is measured by nitrogen adsorption at 77 K using the BET equation (Gemini 2360, Micromeritics). At least 10 m^2 adsorption area is measured for each sample to ensure accuracy. The particle morphology is characterized by transmission electron microscopy (TEM, Philips EM 400 operating at 100 kV). Assuming spherical particles, the average primary particle size d_p is calculated from the measured specific surface area A and particle density ρ_p by $d_p = 6/\rho_p A$ (ρ_p equals 2.2 and 7.0 g/cm^3 for SiO_2 and SnO_2, respectively). The primary particle sizes calculated from BET-adsorption areas are usually larger than their TEM sizes as necks between particles increase the BET size. The flame temperature is measured with a 0.015-in. (0.381-mm) Pt-Rh R-type thermocouple (Omega Engineering) in the absence of a precursor (to avoid particles deposit on the thermocouple tip) but with the corresponding carrier gas Ar flowing through the burner. All flame temperatures are corrected for radiation losses (Collis and Williams, 1959). The product powder mass is determined by weighing the loaded filters on a balance (Mettler AE50).

Results and Discussion

Flame characteristics

Two flame configurations are investigated: a standard and an inverse diffusion flame. In both flame configurations, Ar gas saturated with the precursor vapor passes through the central tube of the reactor. The oxidant/methane flow rates and adiabatic temperature of each reactant mixture are identical, but the stream positions are varied. In the inverse diffusion flame (IDF), oxidant and fuel are introduced through the second and third tube of the reactor, respectively, while in the standard diffusion flame (DF), oxidant and fuel positions are exchanged (Figure 1). In combustion terminology, the IDF has two flame fronts, an internal front between the supplied oxidant and methane streams and an external one between methane and the surrounding still air. In contrast, the DF has only one external flame front between the supplied oxidant and methane streams. The DF has been studied extensively for soot formation during fuel combustion (Santoro et al., 1987; Skaggs and Miller, 1995; Du and Axelbaum, 1995) while limited studies on the IDF have been carried out.

Diffusion flames exhibit strong gradients in concentration and temperature during particle formation and growth. Changes in the initial conditions of the fuel or oxidant affect the flame temperature, particle concentration and velocity, and as a result the product particle size and morphology. Figure 2 shows the maximum temperature of each flame using either air (Figure 2a) or pure oxygen (Figure 2b) as oxidant. The maximum temperatures of the oxygen flames are up to 750 K higher than those of air flames since nitrogen in air is inert and dissipates heat. The temperature of the IDF is lower than that of the DF with both oxidants. The IDF exhibits two flame fronts dissipating the generated heat much faster than the single diffusion flame (DF). As a result, the IDF does not

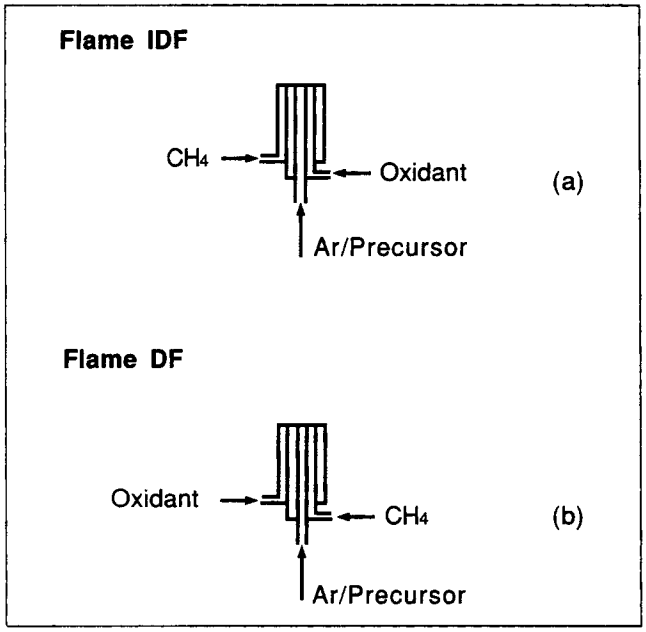

Figure 1. Reactant mixing configurations: (a) inverted diffusion flame (IDF); (b) standard diffusion flame (DF).

reach as high a temperature as the DF. As the air-flow rate increases from 2,500 to 5,500 cm^3/min, the flame temperatures increase steadily since higher air-flow rates provide additional O_2 so that complete combustion takes place faster in the flame. In contrast, with increasing oxygen flow rate, the flame temperatures increase up to 3,800 cm^3/min oxygen and then decrease because complete combustion is reached quickly even at the lowest oxygen flow rate. As a result, additional oxygen (5,500 cm^3/min) dissipates the generated heat and lowers the flame temperature.

Figure 3a shows the axial temperature profile of the standard diffusion flame (DF) along its center line using either air or oxygen as oxidant at a flow rate of 5,500 cm^3/min. The IDF exhibits similar axial temperature profile as the DF for both oxidant gases. It is worth noting that oxygen flames have a much sharper axial temperature gradient than air flames. The luminous region of oxygen flames is rather short (2–4 cm) and close to the burner face. In contrast, the luminous region of air flames starts 1–2 cm away from the burner face and it is about 5–9 cm long. For example, when oxygen is used, the temperature at the burner face can be as high as 1,300 K and the maximum flame temperature (2,050 K) is about 1 cm from the burner face. However, for air flames, the temperature at the burner face is only about 500 K, and the maximum flame temperature region is located at about 4 cm above the burner. Thus, the particle residence time in the high temperature oxygen flames is shorter than that in the air flames.

Figure 3b shows the IDF and DF radial temperature profiles at 1.5 cm above the burner face with oxygen as oxidant. For the DF, the highest temperature region is located near the center line of the flame, which is qualitatively similar in appearance to the previously reported temperature profile by Skaggs and Miller (1995) using tunable diode laser absorption spectroscopy (TDLAS) measurements. In the IDF, however, early on the maximum flame temperature is off the burner axis because of the existence of two diffusion flame fronts. More specifically, the highest temperature region is near the internal flame front where methane and the flowing oxidant stream meet (about 0.8 cm from the center line at this axial height). Using air as oxidant results in similar radial

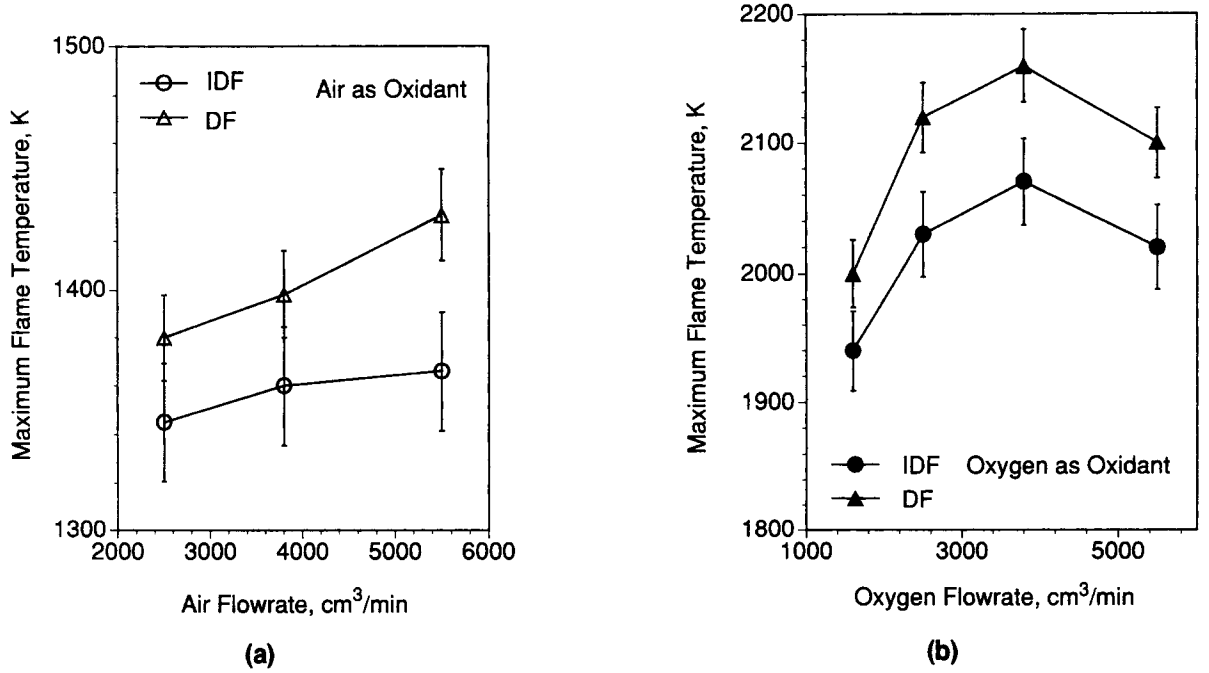

Figure 2. Maximum flame temperature in the IDF and DF configurations using: (a) air; (b) oxygen as oxidant with 400-cm^3/min CH_4 and 250-cm^3/min Ar.

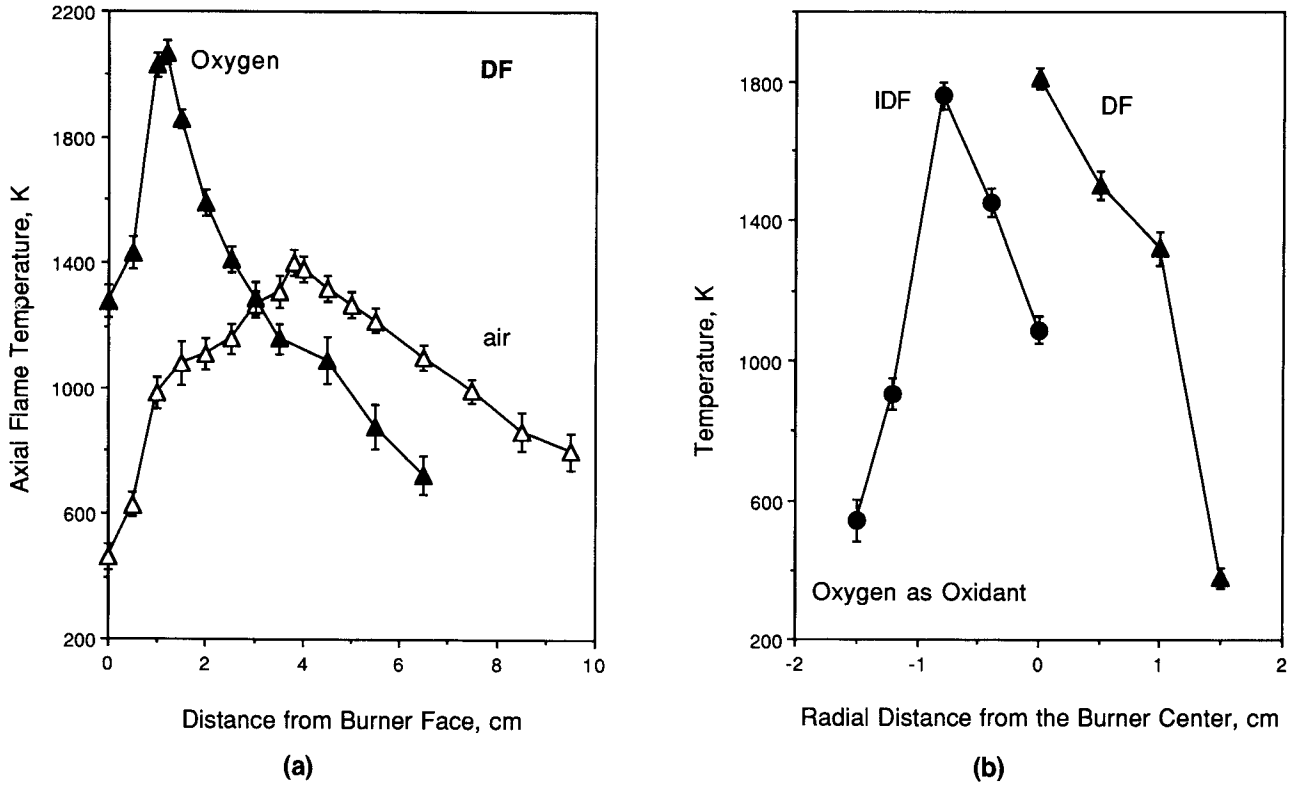

Figure 3. (a) Axial temperature profiles of the DF using air (open symbols) and pure oxygen (filled symbols) as oxidant at 5,500 cm^3/min; (b) radial temperature profiles at 1.5 cm above the burner mouth in configuration IDF and DF using oxygen as oxidant.

Gas flow rates through the burner are CH_4 400 cm^3/min, Ar 250 cm^3/min, and oxidant 5,500 cm^3/min.

temperature profiles except that the temperatures are lower and their gradients are less steep than with oxygen as oxidant.

Synthesis of SiO_2

Figure 4 shows TEM pictures of SiO_2 particles made in the DF with air and oxygen as oxidant (3,800 cm^3/min), respectively. The SiO_2 particle size and morphology are greatly affected by the oxidant gas. The primary particle diameter of SiO_2 made in the air flame is 5 times smaller than in the oxygen flames, specifically, 20 nm and 100 nm, respectively, in average. The shape of the particles is also changed from irregular to spherical. These results are attributed to the temperature difference of these two flames (Figure 3a). When oxygen is used as oxidant, the maximum flame temperature is 700 K higher than when air is used. Higher flame temperature enhances the sintering rate of silica and, thus, results in larger particles.

Figure 5 shows the BET average primary particle size of SiO_2 as a function of air (open symbols) or oxygen (filled symbols) flow rate in both flames. Increasing oxidant flow rate increases the surface area of SiO_2 particles in all flames because the gas velocity is enhanced and the flame length is shortened (the combustion rate is increased), and, consequently, the particle residence time at high temperatures is decreased. However, the reduction of particle size with increasing oxidant flow rate is greater in the air flame (reduced by a factor of 1.6–1.8 when the air-flow rate increases from 2,500 cm^3/min to 5,500 cm^3/min) than in the oxygen flames (reduced only by 1.2–1.3 times). Fine particles (~ 20 nm) made in air flames sinter faster than larger ones made in oxygen flames. As a result, the former are more sensitive to flame temperature and residence time. The inverse diffusion flame (IDF) always produces finer SiO_2 particles than the classic diffusion flame (DF) since the temperature in the IDF is lower than in the DF (Figure 2). In addition, the highest temperature region is located close to the center line of the DF through which most of the precursor vapor and newly formed oxide particles pass through and experience effective sintering, thus, generating larger particles. The IDF, however, exhibits two diffusion flame fronts and the maximum flame temperature occurs near the methane and oxidant gas flame front (Figure 3b) during particle formation. Since the temperature at the center line of the flame is lower, a large fraction of the newly formed particles cannot be sintered effectively by passing through the flame, resulting in fine particles.

In the IDF, even though particles made in air flames are smaller than those made in oxygen, the size difference is only 1.3–1.6 times depending on the oxidant flow rate. This is much smaller than the size difference of particles made in air or oxygen with DF: 4.4–6.5 times. Since the trajectory of most particles in the flame is near the center line, the temperature at this region is most important. In the IDF with oxygen as oxidant, aside from a very steep high temperature region at

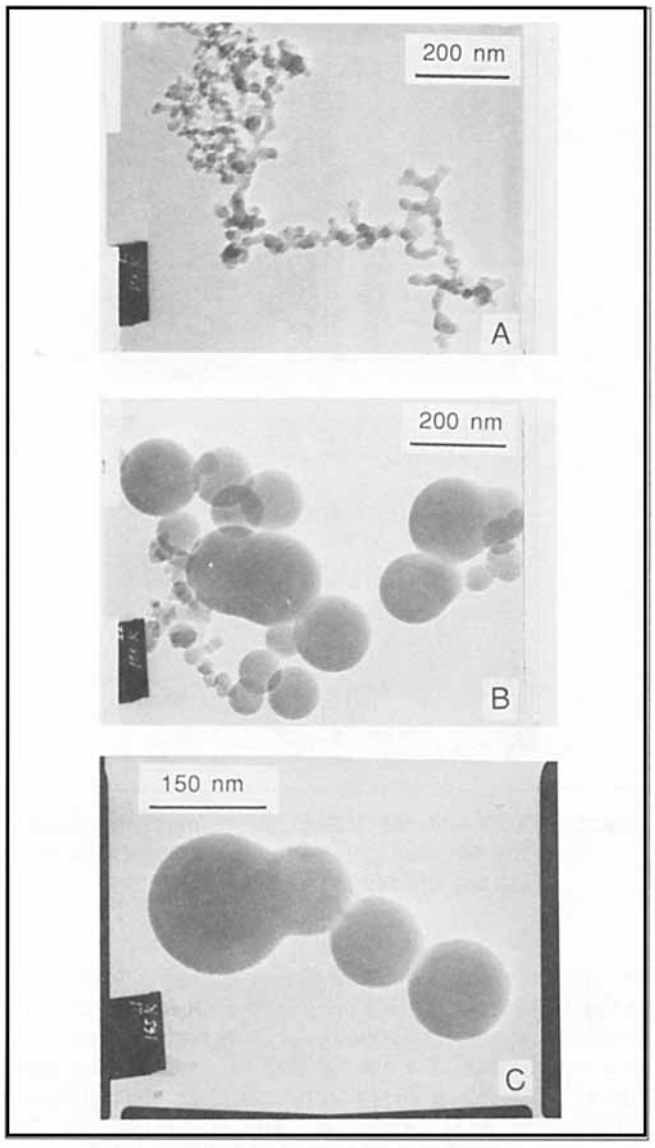

Figure 4. TEM pictures of SiO_2 particles synthesized in the DF using 3,800 cm^3/min of (a) air; (b, c) oxygen as oxidant.

the internal flame front, the center line temperature of the flame is only about 1,100 K (Figure 3b), which is comparable to that of the air flame, 950 K. In the DF, however, there is a significant temperature difference (up to 750 K) between air and oxygen flames at the flame center, where the highest flame temperature region is. Thus, the oxidant, air or oxygen here is more significant for the size of SiO_2 particles made in the DF rather than in the IDF configuration.

In previous work (Zhu and Pratsinis, 1996), TiO_2 particles were synthesized under the same flame conditions as SiO_2 here. No significant difference in the specific surface area of TiO_2 could be detected in the IDF configuration (flames A and B) when different oxidant was used, while there is a significant size difference (1.3–1.6 times) for SiO_2 particles. When the DF was used (flame C in Zhu and Pratsinis, 1996), using oxygen or air as oxidant resulted in TiO_2 particles with a size difference of 2–3 times. This is a bit less than the size

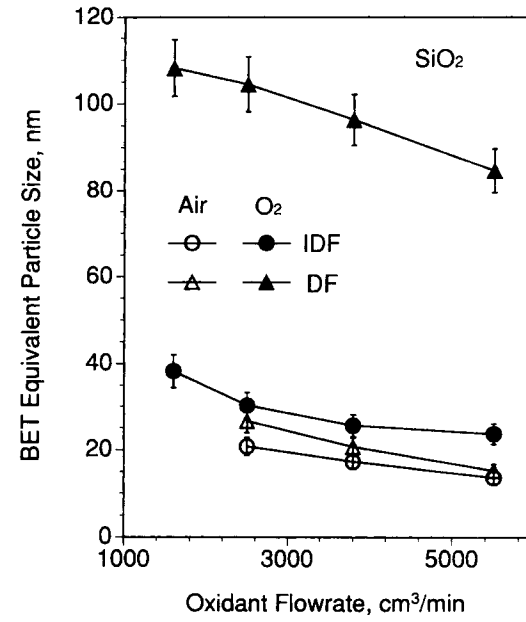

Figure 5. BET equivalent size of SiO_2 particles as a function of oxidant flow rate in the IDF and DF configurations.

difference observed during SiO_2 synthesis in the same flame. Titania sinters much faster than SiO_2 (Akhtar et al., 1992). Ulrich and Riehl (1982) found out that a decrease of only 2% (40 K) in flame temperature was sufficient to cause a surface area increase of SiO_2 up to 25%. They attributed it to the decrease of silica viscosity with temperature in agreement with our data.

Synthesis of SnO_2

Figure 6 shows the BET equivalent primary particle size of SnO_2 synthesized in the IDF (circles) and DF (triangles) as a function of oxidant (air or oxygen) flow rate. As with silica, increasing oxidant flow rate decreases the average primary particle size. This shows that the SnO_2 particle size is affected by flame configuration but not by oxidant composition. The particle diameter is about twice as large when it is made in the DF rather than in the IDF. Even for particles synthesized in the DF configuration, no particle size difference can be found between the particles made in the high-temperature oxygen flame and in the low-temperature air flame. The oxidant has hardly any effect on particle size, probably due to its low melting point of SnO_2 (1,127°C) so that even in the low-temperature air flame, the sintering rate is already fast enough so that particle growth is only affected by the precursor concentration through the oxidant flow rate.

According to Pratsinis et al. (1996), keeping the temperature constant but decreasing the $TiCl_4$ concentration reduces the product TiO_2 particle size. The decrease of the precursor concentration in the flame reduces the initial particle number concentration, resulting in lower coagulation rates and small, loose aggregates with less contact points between the primary particles. Since particle sintering occurs on contact (Koch and Friedlander, 1990), the fusion rate among the primary particles decreases, resulting in smaller individual particles. Here in the IDF configuration, the $SnCl_4$ stream is

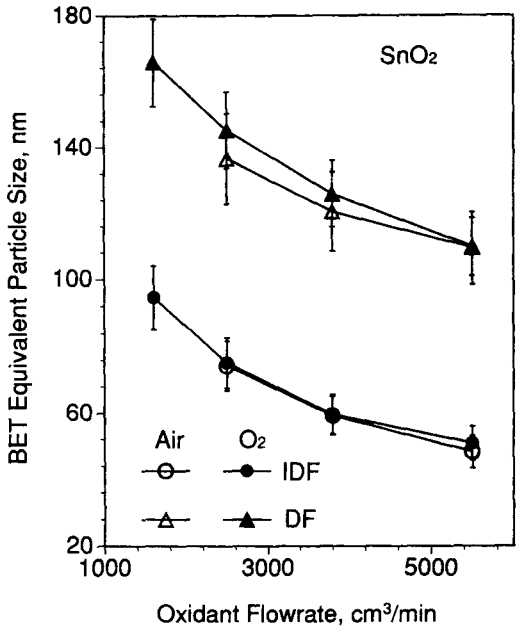

Figure 6. BET equivalent size of SnO_2 particles with respect to oxidant flow rates made in the IDF and DF configurations.

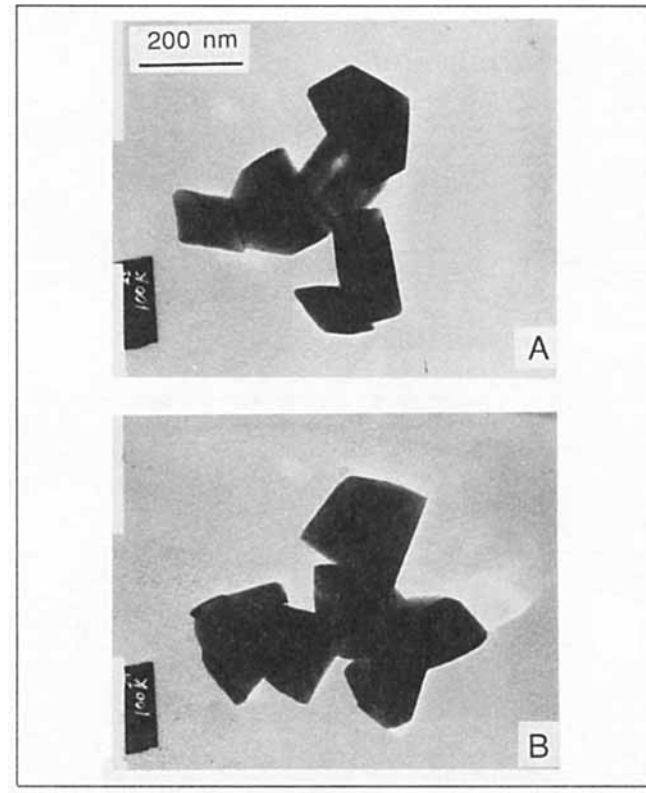

Figure 7. TEM pictures of SnO_2 particles synthesized in the DF configuration using 3,800 cm^3/min of (a) air; (b) oxygen as oxidant.

diluted with oxidant prior to its oxidation in the flame (6–22 times dilution for the oxidant flow rate of 1,600 to 5,500 cm^3/min, respectively). However, in the DF, the dilution of the $SnCl_4$-laden Ar stream with the adjacent CH_4 stream is not that significant since both streams have comparable flow rates 250 and 400 cm^3/min, respectively. As a result, larger SnO_2 particles are made in the DF rather than in the IDF as was observed in the oxygen DF synthesis of SiO_2. Based on the previous discussion, the effect of temperature in the synthesis of SnO_2 particles is not significant at the present flame conditions (or rather high-temperature range). Compared to the DF configuration, the precursor in the IDF is diluted by 3–11 times, resulting in a decrease of 1.8–2.4 times in primary particle size, which is in agreement with TiO_2 flame synthesis data (Pratsinis et al., 1996).

The TEM pictures of SnO_2 particles made in the DF configuration with air and oxygen as oxidant (3,800 cm^3/min) are shown in Figure 7. The morphology of the crystalline stannic oxide particles synthesized in both flames remains faceted in contrast with that of amorphous SiO_2 (Figure 4). Particles grow by collision (coagulation) and coalescence (sintering) in the flame. If sintering is faster, single particles are produced while if collisions are faster, dendritic agglomerates are formed (Fotou et al., 1994b; Lehtinen et al., 1996). Silica sinters by viscous flow and is very sensitive to flame temperature at the employed conditions. At low temperatures, dendritic aggregates consisting of many small particles are formed as the sintering rate is low. At elevated temperatures, large, single and spherical SiO_2 can be made (Figure 4b) although necks can still be seen between some particles. Figure 4c gives a snapshot of the growth mechanism of SiO_2: particles fuse (sinter) as they touch each other while additional material may be added by the reaction on the particle surface (surface growth) of $SiCl_4$. As to the stannic oxide which follows an evaporation condensation sintering mechanism (Harrison and Willet, 1989), particles remain distinct and separate as shown in Figure 7 because the sintering rates are fast enough at the employed experimental conditions. Using either oxygen or air as the oxidant gas, the average particle size stays the same, about 125 nm. When TiO_2 particles are made under the same conditions as SnO_2 particles are made here (Figure 7b), single spherical particles were produced (Zhu and Pratsinis, 1996). However in the current situation, only faceted SnO_2 particles are generated which can be attributed to their differing material properties. Ziemann et al. (1996) studied the morphology of KCl particles generated in a furnace reactor, while Matijevic et al. (1963) investigated the shape transformation of NaCl particles which follow also the evaporation-condensation sintering mechanism. They found that in the presence of water vapor spherical particles were transformed to cubes. Here, it may be possible that the faceted SnO_2 particles are affected (hydrated and recrystallized) by the presence of water generated by methane combustion. This, however, is the subject of a separate study.

Figure 8 shows XRD patterns of flame made stannic oxide powders. While particles synthesized in either IDF or DF are all cassiterite, those made in IDF have broader peaks than DF made ones, indicating finer primary particles are generated in IDF consistent with the above BET measurements.

Conclusions

Nanosized SiO_2 and SnO_2 particles were synthesized in diffusion flame reactors. Two reactant mixing configurations,

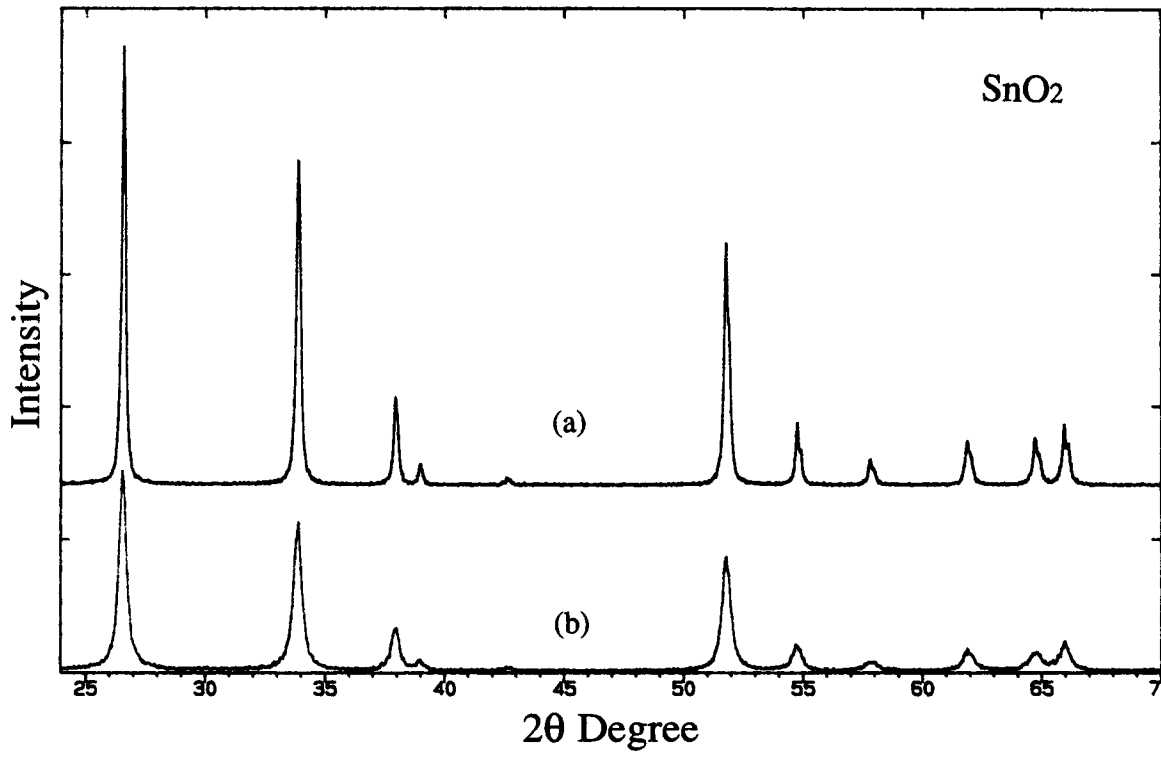

Figure 8. XRD patterns of flame made stannic oxide particles with (a) DF, 3,800 cm^3/min O_2; (b) IDF, 3,800 cm^3/min air.

one with a single diffusion flame front and the other with two diffusion flame fronts were investigated using air or oxygen as oxidants. The maximum temperature of these two flame configurations is located at different regions in the flame, affecting, thus, early particle inception and growth. Oxygen flames result in higher temperature but steeper temperature gradients than air flames. By changing the reactant mixing configuration and oxygen partial pressure in the oxidant, the primary particle size of the oxide powders can be controlled. The different sintering mechanisms and material properties of SiO_2 and SnO_2 result in different primary particle sizes. The oxidant composition has little effect on SnO_2 particle size, while the size of silica particles increases with increasing oxygen ratio in the oxidant stream.

Acknowledgments

We acknowledge support from the Presidential Young Investigator Award (SEP) by the National Science Foundation, CTS-8957042 and more recently, CTS-9612107.

Literature Cited

Akhtar, M. K., S. E. Pratsinis, and S. V. R. Mastrangelo, "Dopants in Vapor-Phase Synthesis of Titania Powders," *J. Amer. Ceramic Soc.*, **75**, 3408 (1992).

Bautista, J. R., and R. M. Atkins, "The Formation and Deposition of SiO_2 Aerosols in Optical Fiber Manufacturing Torches," *J. Aerosol. Sci.*, **22**, 667 (1991).

Clark, H. B, "Titanium Dioxide Pigments," in *Treatise on Coatings*, Vol. 3, R. R. Myers and J. S. Long, eds., Marcel Dekker, New York, p. 479 (1975).

Collis, D. C., and M. J. Williams, "Two-Dimensional Convection from Heated Wires at Low Reynolds Numbers," *J. Fluid Mechanics*, **6**, 357 (1959).

Du, J., and R. L. Axelbaum, "The Effect of Flame Structure on Soot-Particle Inception in Diffusion Flames," *Comb. and Flame*, **100**, 367 (1995).

Fotou, G. P., S. Vemury, and S. E. Pratsinis, "Synthesis and Evaluation of Titania Powders for Photodestruction of Phenol," *Chem. Eng. Sci.*, **49**, 4939 (1994a).

Fotou, G. P., S. E. Pratsinis, and P. A. Baron, "Coating of Silica Fibers by Ultrafine Particles in a Flame Reactor," *Chem. Eng. Sci.*, **49**, 1651 (1994b).

Fotou, G. P., S. J. Scott, and S. E. Pratsinis, "The Role of Ferrocene in Flame Synthesis of Silica," *Comb. and Flame*, **101**, 529 (1995).

Formenti, M., F. Juillet, P. Meriaudeau, S. J. Teichner, and P. Vergnon, "Preparation in a Hydrogen-Oxygen Flame of Ultrafine Metal Oxide Particles," *J. Colloid Inter. Sci.*, **39**, 79 (1972).

Harrison, P. G., and M. J. Willett, "Tin Oxide Surfaces," *J. Chem. Soc., Faraday Trans. 1*, **85**, 1921 (1989).

Koch, W., and S. K. Friedlander, "The Effect of Particle Coalescence on the Surface Area of a Coagulating Aerosol," *J. Colloid Inter. Sci.*, **140**, 419 (1990).

Lehtinen, K. E. J., R. S. Windeler, and S. K. Friedlander, "Prediction of Nanoparticle Size and the Onset Dendrite Formation Using the Method of Characteristic Times," *J. Aerosol Sci.*, **27**, 883 (1996).

Matijevic, E., W. F. Espenscheid, and M. Kerker, "Aerosols Consisting of Spherical Particles of Sodium Chloride," *J. Colloid Sci.*, **18**, 91 (1963).

Matsoukas, T., and S. K. Friedlander, "Dynamics of Aerosol Agglomerate Formation," *J. Colloid Inter. Sci.*, **146**, 495 (1991).

Perry, R. H., D. W. Green, and J. O. Maloney, eds., *Perry's Chemical Engineers' Handbook*, McGraw-Hill, New York (1984).

Pratsinis, S. E., "Flame Aerosol Synthesis of Ceramic Powders," *Prog. Energy Combust. Sci.*, in press (1997).

Pratsinis, S. E., and S. V. R. Mastrangelo, "Material Synthesis in Aerosol Reactors," *Chem. Eng. Prog.*, **85**, 62 (1989).

Pratsinis, S. E., W. Zhu, and S. Vemury, "The Role of Gas Mixing in Flame Synthesis of Titania Powders," *Powder Technol.*, **86**, 87 (1996).

Santoro, R. J., T. T. Yeh, J. J. Horvath, and H. G. Semerjian, "The

Transport and Growth of Soot Particles in Laminar Diffusion Flames," *Comb. Sci. and Tech.*, **53**, 89 (1987).
Skaggs, R. R., and J. H. Miller, "A Study of Carbon Monoxide in a Series of Laminar Ethylene/Air Diffusion Flames Using Tunable Diode Laser Absorption Spectroscopy," *Comb. and Flame*, **100**, 430 (1995).
Ulrich, G. D., "Theory of Particle Formation and Growth in Oxide Synthesis Flames," *Comb. Sci. Tech.*, **4**, 47 (1971).
Ulrich, G. D., and J. W. Riehl, "Aggregation and Growth of Submicron Oxide Particles in Flames," *J. Colloid and Inter. Sci.*, **87**, 257 (1982).
Vemury, S., and S. E. Pratsinis, "Dopants in Flame Synthesis of Titania," *J. Amer. Ceram. Soc.*, **78**, 2984 (1995a).
Vemury, S., and S. E. Pratsinis, "Corona-Assisted Flame Synthesis of Ultrafine Titania Particles," *Appl. Phys. Lett.*, **66**, 3275 (1995b).
Weast, R. C., ed., *CRC Handbook of Chemistry and Physics*, 64th ed., CRC Press, Boca Raton, FL, p. D197 (1983).
Zachariah, M. R., and S. Huzarewicz, "Aerosol Processing of YBaCuO Superconductors in a Flame Reactor," *J. Mater. Res.*, **6**, 264 (1991).
Zhu, W., and S. E. Pratsinis, "Flame Synthesis of Nanosize Particles: Effect of Flame Configuration and Oxidant Composition," *Nanotechnology: Molecularly Designed Materials*, ACS Symp. Ser., G.-M. Chow and K. E. Gonsalves, eds., **622**, 64 (1996).
Zhu, W., "The Role of Reactant Mixing in Flame Synthesis of Nanosize Ceramic Powders," MS Thesis, Univ. of Cincinnati (1996).
Ziemann, P. J., D. B. Kittelson, and P. H. McMurry, "Effects of Particle Shape and Chemical Composition on the Electron Impact Charging Properties of Submicron Inorganic Particles," *J. Aerosol Sci.*, **27**, 587 (1996).

Manuscript received Oct. 28, 1996, and revision received May 5, 1997.